JOURNAL OF AGRICULTURAL AND FOOD CHEMISTRY

Article

pubs.acs.org/JAFC

Detection of Engineered Silver Nanoparticle Contamination in Pears

Zhong Zhang,[†] Fanbin Kong,[‡] Bongkosh Vardhanabhuti,[†] Azlin Mustapha,[†] and Mengshi Lin*[,†]

[†]Food Science Program, Division of Food Systems & Bioengineering, University of Missouri, Columbia, Missouri 65211-5160, United States

[‡]Department of Food Science & Technology, University of Georgia, Athens, Georgia 30602-7610, United States

ABSTRACT: Engineered nanomaterials such as silver nanoparticles (Ag NPs) have been increasingly used in agriculture owning to their antimicrobial and insecticidal properties. However, the contamination of Ag NPs in foods and water may pose a great risk to public health and the environment. In this study, the contamination of Ag NPs in pears was detected, characterized, and quantified by a combination of techniques, including transmission electron microscopy (TEM), scanning electron microscopy (SEM), energy dispersive spectrometer (EDS), and inductively coupled plasma optical emission spectrometry (ICP-OES). Pear samples were treated with two different sizes (20 and 70 nm in diameter) of Ag NPs and stored for different times. Quantification results of Ag NPs in pear samples by ICP-OES demonstrate that there is a good linear relationship (R^2 = 0.983) between the spiked values and recovered values. Residual Ag NPs of both 20 and 70 nm were still detected in samples after 4-day treatment followed by rinsing with water. The penetration study reveals that 20 nm Ag NPs might penetrate the pear skin and pulp after 4-day treatment, while this phenomenon was not observed for 70 nm Ag NPs. These results demonstrate that a combination of techniques could provide accurate results for detection, characterization, and quantification of engineered nanoparticles in agricultural products.

KEYWORDS: *Ag nanoparticles, TEM, SEM, ICP-OES, pear*

INTRODUCTION

It is estimated that global crop yields are reduced by 20 to 40% per year due to pest infection and plant diseases.[1,2] The use of pesticides could effectively control this problem and improve the quality of crops.[3] In recent years, inorganic pesticides, such as nanosized silver, silica, and copper, have captured the attention of agrichemical companies. In particular, silver nanoparticles (Ag NPs), known for their antimicrobial and insecticidal properties, have been used as pesticides in agriculture or intentionally incorporated in food packaging materials.[4] By doing so, the manufacturers expect that new products can help farmers spray the fields more efficiently and release less pesticide to environmental drift and stormwater runoff. However, the toxicity of nanoscale pesticides to humans and the environment has not been fully investigated and understood.[5,6] There is little information about the fate of these nanosilver pesticides in the environment or in agriculture products. Therefore, there is a growing concern about the safety of nanosilver pesticides used in food crops and produce.

To understand the fate and measure the residue of nanosilver in food crops, it is critical to have a suitable and accurate analytical method for detection and characterization of Ag NPs. However, little information could be found on detection and characterization of Ag NPs in agricultural products. Because no single technique is able to provide all the information that is necessary to identify and quantify Ag NPs in food crops, we aimed to develop a combination of methods that are sensitive enough for the measurement of low concentrations of Ag NPs and that can directly observe the size, shape, and translocation of Ag NPs in fruit samples.

Conventional techniques such as optical microscope are unsuitable for measuring extremely small size of NPs. Several studies have been reported on the detection of NPs using field flow fractionation (FFF), hydrodynamic chromatography (HDC), and dynamic light scattering (DLS).[7−9] Although FFF, HDC, and DLS are good methods to detect the size distribution of NPs, they require suspending NPs in solution prior to testing, and it is difficult to apply these methods in detection of NPs in foods due to the difficulty in extracting the NPs from food matrices, especially when the concentration of NPs is at a very low level. In addition, these methods cannot be used to measure important physical properties (shape, etc.) of NPs and the interaction between NPs and plant tissues. In this study, TEM and SEM were selected to detect the Ag NPs in fruits because they have been widely used to characterize the size, shape, and structure of nanomaterials and can directly detect and visualize the penetration and interaction of NPs with plant tissues.[10−13] In addition, inductively coupled plasma optical emission spectrometry (ICP-OES) has been employed to determine the metal content in the soil and plant samples with high accuracy.[14] Different metal elements could be rapidly detected by ICP-OES at one time.[15,16] ICP-OES were thus selected in this study to determine the concentration of Ag NPs in fruit samples.

The objective of this study was to detect, characterize, and quantify Ag NPs in fruit samples (i.e., pears) by a combination of techniques including TEM, SEM, EDS, Zetasizer, and ICP-OES. The residue and penetration of Ag NPs on the pear skin were studied by TEM, SEM, and ICP-OES.

Received: August 8, 2012
Revised: October 10, 2012
Accepted: October 10, 2012
Published: October 19, 2012

dx.doi.org/10.1021/jf303423q | *J. Agric. Food Chem.* 2012, 60, 10762−10767

MATERIALS AND METHODS

Pear Samples and Ag NPs. Pears were purchased from a local grocery store. Ag NPs were purchased from NanoComposix (San Diego, CA, USA) with a silver concentration of 0.02 mg/mL in citrate solution and an average diameter of 20 and 70 nm, respectively. Ag NPs with different diameters were used in this study due to the fact that most nanoscale silver was present as mixed nanoparticles in the pesticide solutions. The size distribution of NPs was measured by a Zeta-sizer (Malvern Nano S, Worcestershire, U.K.). TEM (JEOL 1400, Tokyo, Japan) and SEM equipped with EDS (Quanta FEG 600 ESEM) were used to characterize the Ag NPs in the pear tissues. The size of Ag NPs was calculated using ImageJ 1.45 (available at http://rsb.info.nih.gov/ij/).

TEM Characterization of Ag NPs in Pear. A pear skin (4.7 mm^2) and a pulp cube (2 mm × 2 mm × 1 mm) were cut from the pear and immersed in the Ag NP (20 nm) solution for 5 days. The specimens were then washed with distilled water and suspended in a primary fixative solution (2% glutaraldehyde, 2% paraformaldehyde in 0.1 M cacodylate) for 2 h on a rocker at room temperature. The specimens were washed three times with buffer and placed into a secondary fixative solution (2% osmium tetroxide in 0.1 M cacodylate) for 2 h. After the secondary fixation, the specimens were washed three times with distilled water. Dehydration of samples was performed in graded acetone series by the following sequence: 25%, 50%, 70%, and 95% (each for 30 min) and 100% (three times of 30, 30, and 60 min). The infiltration was started using 1 part resin and 2 parts acetone for 2 h, continued with 1 part resin and 1 part acetone for 2 h, 2 parts resin and 1 part acetone for 2 h, and, finally, pure resin for 8 h. The resin was then placed in embedding capsules and polymerized at 60 °C for 2 days. The ultrathin sections were cut and placed on the grid for staining. The grid was stained by uranyl acetate followed by washing with distilled water and lead citrate staining. Finally, the grid was washed by distilled water and observed by TEM (120 kV).

SEM Characterization and EDS Analysis of Ag NPs in Pear Samples. Pear skin and pulp were treated as described in the TEM section. The samples were transferred into the primary fixative solution and then subjected to dehydration, followed by the critical point drying using liquid carbon dioxide. The samples were first flushed by liquid carbon dioxide for 20 min in a critical point drier (AutoSamdri 815, Tousimis, USA). Liquid carbon dioxide was heated above 31 °C and stabilized for 4 min. Then the pressure was gradually released for the drying of pear samples. The skin and pulp samples were then coated with a 150 nm carbon layer for SEM characterization. The elemental composition of embedded NPs in pear tissues was determined by the EDS.

Quantification of Ag NPs in Pear Samples. Pear cubes including the pear skin (50 g) were cut from intact pears. Ag NP solutions with a series of volumes (0 to 1000 μL) were applied on the surface of pear cubes. The pear cubes were then blow-dried at room temperature and stored at 4 °C for 7 days. After storage, the pear cubes were dried at 105 °C for 3 days to completely remove the moisture of the pears. Dried samples were transferred to crucibles and burned at 500 °C for 5 h. After cooling, 10 mL of HCl (6 M) was added in the crucibles to dissolve the ashes. The mixtures were thoroughly transferred to Kimax glass tubes and finally diluted to 50 mL with distilled water. The solution was filtered through Whatman #42 filter papers and subjected to the ICP-OES analysis. The concentration of Ag NPs was expressed as the concentration of Ag element in the pear samples. The recovery rate of Ag NPs was calculated according to the following equation:

$$\text{recovery} = (C_{\text{sample}} - C_{\text{control}})/C_{\text{spiked}} \times 100\% \quad (1)$$

where C_{sample} is the Ag concentration in the spiked pear samples, C_{control} is the Ag concentration in the control pear samples, and C_{spiked} is the concentration of spiked Ag calculated according to the spiked amount of Ag NP solution and the weight of pear samples.

Penetration Studies of Ag NPs on the Pear Skin. A circle (6.7 cm^2) was drawn by an ink pen on the skin of an intact pear. An aliquot (100 μL) of Ag NP solution was dropwise added on the circled skin by a 10 μL pipet. The treated pears were blow-dried at room temperature, sealed in beakers, and then stored in a 4 °C refrigerator. Before sampling, the pear was completely rinsed with deionized water to remove the weakly attached Ag NPs. Both skin and pulp (4.60 ± 0.02 g) under the circled area were carefully peeled and collected from intact pears with time intervals of 0, 2, 4, 6, and 8 days. The concentration of Ag NPs in pear samples was determined by ICP-OES and expressed as the concentration of Ag element. The pretreatments and ICP-OES analysis were similar to the procedure described above.

Data Analysis. Partial least-squares (PLS) linear regression analysis and significance test ($P < 0.05$) were performed using the SPSS software (Version 16.0 for windows, IBM, New York, USA). The detection limit (DL) for Ag NPs was determined and expressed as the concentration of Ag element, which was calculated by the following equation according to the definition from the International Union of Pure and Applied Chemistry (IUPAC):

$$\text{DL} = 3\delta/m \quad (2)$$

where δ is the standard error in the y-intercept, m is the slope obtained from a standard linear regression analysis, and the number 3 represents a 99.86% confidence interval.

RESULTS AND DISCUSSION

Characterization of Ag NPs in Citrate Solution. The size, shape, and other physical properties of Ag NPs (20 and 70 nm) in 2 mM citrate solution were investigated by TEM (Figure 1). It is obvious that silver NPs were uniformly

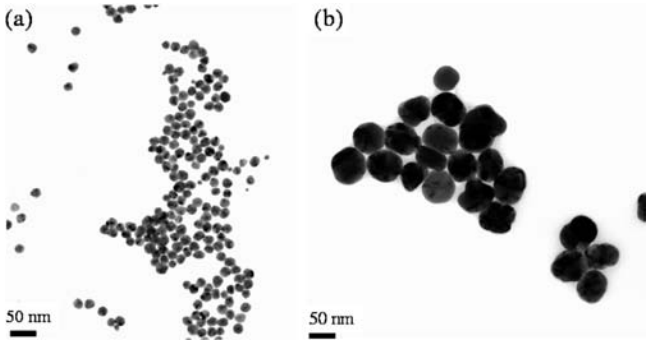

Figure 1. TEM images of Ag NPs in citrate solution: (a) 20 nm; (b) 70 nm.

dispersed in the citrate solution without any agglomerations. The shape of most 20 nm silver NPs was spherical while the 70 nm silver NPs were mostly oval in shape. The TEM image indicates an average particle size of ~21.3 nm and ~69.1 nm for these two types of Ag NPs, respectively, which is in close accordance with the product specifications (20 and 70 nm) provided by the manufacturer. However, TEM is not an ideal technique for routine analysis of size distribution of engineered nanoparticles because it is complicated and expensive. In this study, the size distribution of Ag NPs was also measured by the Zetasizer due to the simplicity and rapidness of this method. Figure 2 shows the size distribution of Ag NPs analyzed by the Zetasizer, which demonstrates that the average size for two types of Ag NPs is 25 and 73 nm, respectively. These results were also close to the labeled diameter provided by the manufacturer. However, the relative standard deviation of 20 nm silver NPs (20%) is larger than that of 70 nm silver NPs (4.2%). This is mainly because the hydrated layer was regarded as part of the silver NPs. Therefore, the results acquired by the Zetasizer exhibit greater relative standard deviation. The advantage of using the Zetasizer is that the size distribution

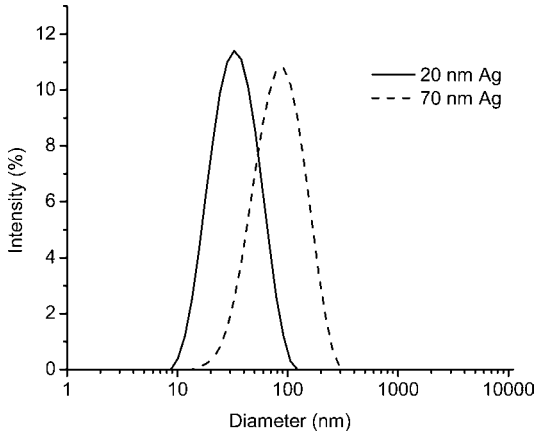

Figure 2. Size distributions of Ag NPs (20 and 70 nm) determined by Zetasizer.

and average diameter of NPs could be directly read from the machine.

Characterization of Ag NPs in Pear Tissues by TEM. Figure 3 shows TEM images in a vertical section of pear tissue samples treated by Ag NPs (20 nm). Ag NPs could be clearly observed in these TEM images. It was found that Ag NPs penetrated into the pear skin from the inner side or outer side of skin via the gaps of skin tissues. Ag NPs were firmly attached in tissues due to the high surface area of Ag NPs. During the penetration process from the surface to the central parts, Ag NPs might lose the protection from surfactant citrate and tended to aggregate due to the interactions with the components in the pear skin. The aggregation status of Ag NPs was clearly observed in Figure 3b. Most Ag NPs were still round in shape, but they aggregated with each other to form a cluster attaching on the pear tissues. Similarly, the penetration of Ag NPs inside the pear pulp was also observed by the TEM (Figure 3c). The size of Ag NPs was around 20 nm, which agrees with the value determined by Zetasizer. The TEM images also show that there was a thick layer coating on Ag NPs inside the pulp tissues (Figure 3d). This may be caused by the interaction of Ag NPs with macromolecular substances such as polysaccharides or pectin in the pear pulp. To detect the contamination of Ag NPs in fruits, it is of great importance to investigate the penetration of Ag NPs inside fruit tissues rather than the surface contamination because those penetrated Ag NPs could not be simply removed by washing with water. TEM could provide visual images for such contamination and penetration in fruit samples. The 20 nm Ag NPs are much smaller than 70 nm Ag NPs and, thus, are more difficult to be detected and visualized in TEM and SEM analysis. If 20 nm Ag NPs could be detected by SEM and TEM, then the same type but with much bigger size of NPs would be easily detected.

Characterization of Ag NPs in Pear Tissues by SEM and EDS. Ag NPs on the surface of pear tissues could be clearly observed by SEM (Figure 4). Due to the high molecular weight of silver element, Ag NPs could be clearly differentiated from pear tissues because backscattered electrons made Ag NPs

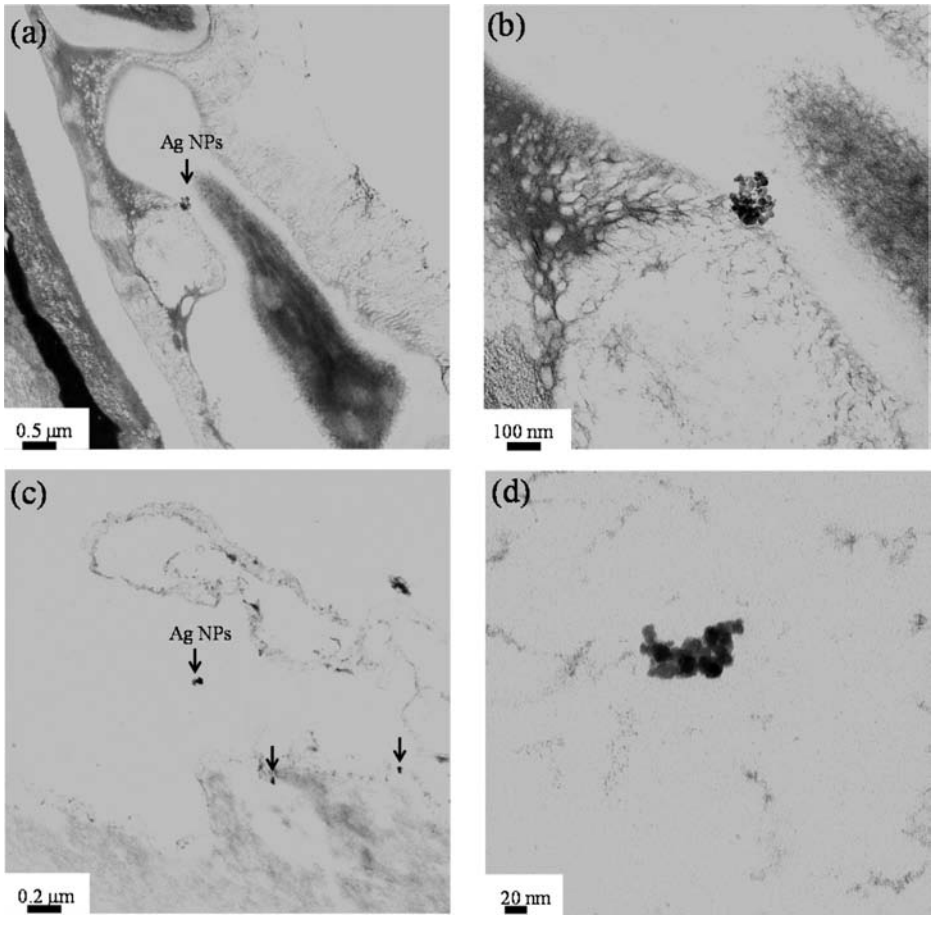

Figure 3. TEM characterizations of Ag NPs on pear tissues: (a, b) pear skin at different magnifications; (c, d) pear pulp at different magnifications.

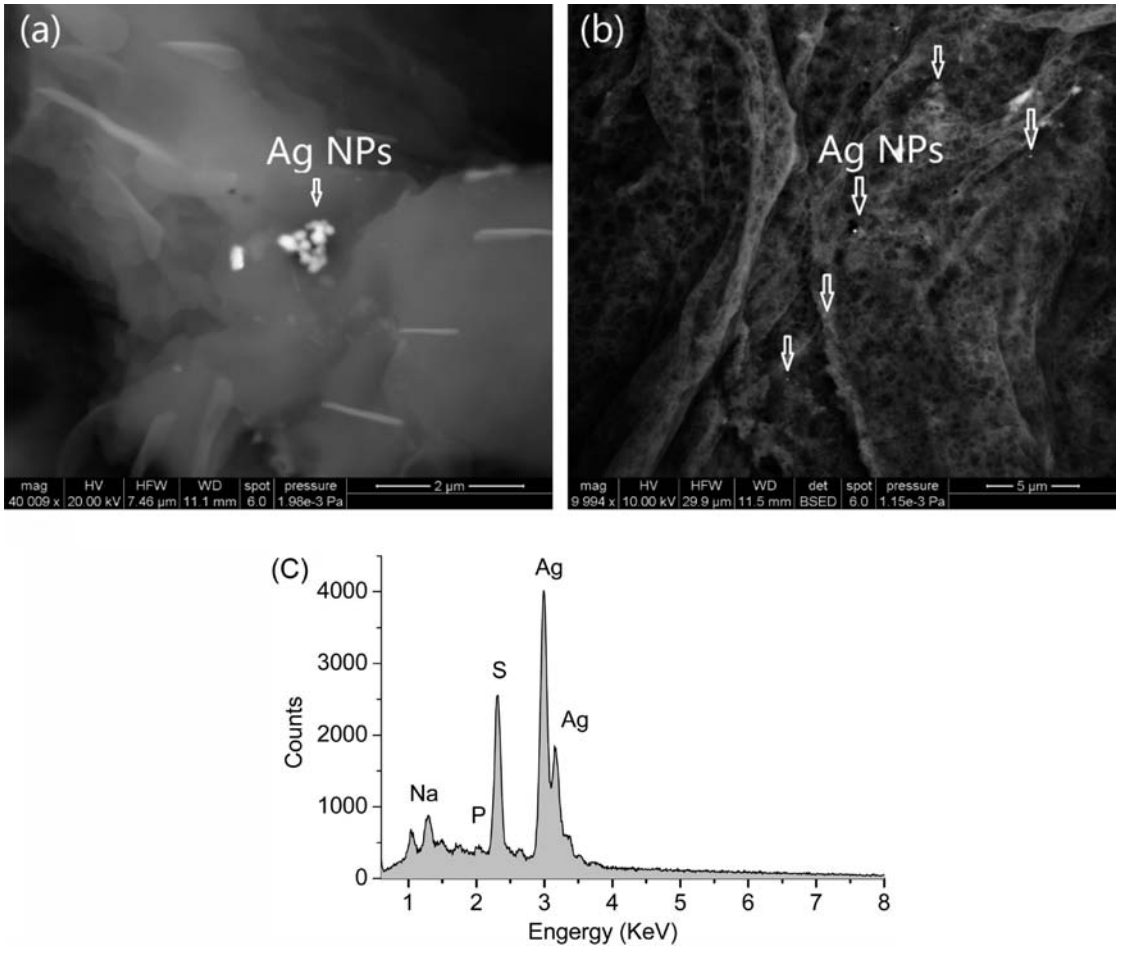

Figure 4. SEM characterizations of Ag NPs on pear tissues: (a) pear skin; (b) pear pulp; (c) a typical EDS profile for the nanoparticles attached on pear skin.

brighter than pear tissues. As shown in Figure 4a, some Ag NPs were coagulated and attached on the surface of pear skin, while other Ag NPs were embedded in the skin tissues. Figure 4b shows the Ag NPs in pear pulp. Some of them were entrapped inside the pulp tissues, thus part of the backscattered electrons were blocked by the pulp tissues, which made them appear darker than other Ag NPs. In addition, the EDS was used to determine the elemental composition of those NPs. It was found that bright dots consisted of different amounts of Ag element ranging from 30% to 72%. The profile of EDS shows that a significant amount of Ag, S, P, and Na was present around the bright dot (Figure 4c). The P and Na are naturally existing elements in pear samples. Therefore, it was concluded that those NPs were Ag NPs. These results demonstrate that SEM coupled with EDS could be used not only to characterize the shape and aggregation status of NPs but also to determine detailed elemental composition of the NPs in fruit samples.

Quantification of Ag NPs in Pears by ICP-OES. The concentrations of silver element in pear samples, contributed by the added silver NPs and naturally existing silver in the pear, were determined by ICP-OES. Trace amounts of silver might be naturally present in pears due to the adsorption of silver from water and soil. As expected, 45.0 $\mu g \cdot kg^{-1}$ of silver was detected in the control samples. As shown in Figure 5, there is a linear relationship between the added values and the predicted values by ICP-OES, and it is evident that the recovered values of Ag NPs were all very close to the spiked values. The slope is

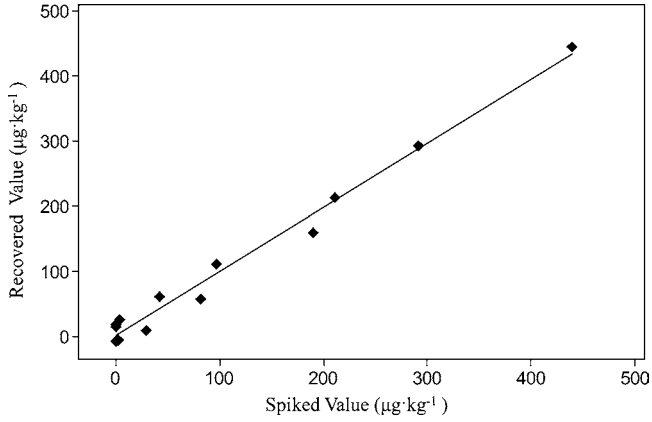

Figure 5. PLS regression fitting between the concentration predicted by ICP-OES and the spiked amount of Ag NPs in the pear samples ($Y = 1.03X - 44.7$, $R^2 = 0.983$, RMSEP = 7.8).

1.03, and R^2 value is 0.983, indicating a good linearity and reliable prediction of this method. The detection limit of this method is 22.7 $\mu g \cdot kg^{-1}$ for silver NPs in pear samples. In the recovery study, the concentration of Ag element in control samples was deducted accordingly because the naturally occurring Ag element in pear samples could contribute to the recovery rate. The recovery of Ag NPs was between 92.3% and 108.2% for the spiked samples (Table 1). The satisfactory

dx.doi.org/10.1021/jf303423q | J. Agric. Food Chem. 2012, 60, 10762−10767

recovery rate demonstrates that ICP-OES is a reliable method to quantify Ag NPs in pear samples.

Table 1. Recovery of Ag NPs in Pear Samples Determined by ICP-OES

spiked ($\mu g \cdot kg^{-1}$)	quantified ($\mu g \cdot kg^{-1}$)	recovery (%)
35.6	38.2 ± 4.3	108.2
92.9	91.7 ± 10.5	98.7
200.7	185.3 ± 6.6	92.3
297.3	310.7 ± 8.1	104.5
419.5	404.3 ± 15.9	96.4

Penetration Studies of Ag NPs on the Pear Skin by ICP-OES. To simulate a real world situation of applied pesticides being washed off by rainwater, Ag NPs (20 and 70 nm) were applied on pears followed by thorough rinsing with deionized water. Figure 6 shows the relative content of silver

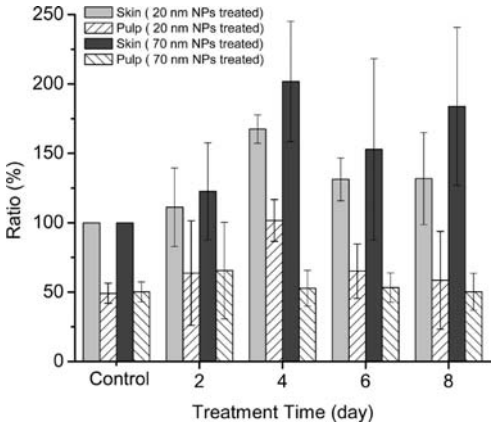

Figure 6. Relative content of Ag (20 and 70 nm) applied on the pear samples under different treatment time (ratio = $C_{sample}/C_{control}$, where C_{sample} represents the concentration of Ag in samples and $C_{control}$ is the Ag concentration of pear skin in the control group).

NPs in pear skin and the underneath pulp in different treatment times. The control samples were untreated pear skin and pulp, which were used to compare the accumulation and penetration of Ag NPs in treated samples. There is a significant difference in Ag content between the skin and pulp in the control group ($P < 0.05$). This is reasonable because the pear skin was directly exposed in the environment and was apt to adsorb the contaminants from the environment such as soil and air. The amounts of Ag in pear skin were enhanced by the treatment of Ag NPs after 4-day storage for both 20 and 70 nm Ag NPs. This indicates that some silver NPs were firmly attached on pear skins after 4-day treatment and could not be removed by rinsing with water. But other weakly attached Ag NPs could be carried away by rainwater and migrate to the environment, thus contaminating the soil and water. For pear samples per se, the residual Ag NPs on pear skin might not cause health problems to consumers because usually the pear skin is peeled off before consumption. Therefore, it would be interesting to investigate if Ag NPs could penetrate the pear skin and into the pulp.

The pear pulp right under the treated skin was sampled and subjected to ICP-OES measurement. The results show that the Ag content in the pulp increased by 50% four days after the treatment with 20 nm Ag NPs, indicating the potential penetration of Ag NPs into the pear pulp. This characteristic of silver NPs is dangerous to consumers because NPs could translocate in the human body via direct digestion of pear pulps in the gastrointestinal tract.[17] The Ag content in the pulp was slightly reduced after 6-day and 8-day treatments, which may be caused by further penetration of Ag NPs into the pear pulp or the translocation of Ag NPs to the surrounding pulp tissue. However, no increase was observed in the pear pulp samples treated with 70 nm Ag NPs. The concentration of 70 nm Ag NPs in the pear pulp maintained at the same level as that of the control even 8 days after the treatment. This may be due to the fact that 20 nm Ag NPs have a much smaller particle size than 70 nm NPs, which facilitated the penetration of Ag NPs into pear skin and translocation to the pulp. This phenomenon agrees with other studies about the penetration of Ag NPs into the cell wall of bacteria.[18,19] Previous studies have shown that the antibacterial ability of smaller NPs is much stronger than that of larger NPs due to the easier penetration of smaller NPs. Therefore, smaller NPs may be more harmful to consumers than larger counterparts. From this standpoint, the use of nanosilver pesticides in food crops should be carefully regulated.

In summary, the contamination of Ag NPs in pears was investigated in this study. The size, shape, and other properties of Ag NPs in solution or in pear tissues were characterized by Zetasizer, TEM, SEM, and EDS. The quantification of Ag NPs in pear samples was performed by ICP-OES. There was a good linear relationship between the recovered and spiked values of Ag NPs ($R^2 = 0.983$) with a detection limit of 22.7 $\mu g \cdot kg^{-1}$, demonstrating that ICP-OES is an accurate method for quantification of Ag NPs in pear samples. Moreover, the attachment and penetration of Ag NPs in pears were also investigated in this study. It was found that both 20 and 70 nm Ag NPs were still attached on the pear skin after 4 days of treatment followed by rinsing with deionized water. The results reveal that 20 nm Ag NPs could penetrate the pear skin and pulp, while 70 nm Ag NPs did not. This study provides a promising approach for detection, characterization, and quantification of Ag NPs in food crops or other agricultural products. Compared with other methods such as FFF, HDC, and DLS, the advantage of the proposed method using a combination of techniques is that it can not only detect, characterize, and quantify Ag NPs but also directly visualize the penetration of NPs in food tissues. Future research is needed to study the contamination and penetration of different type of nanoparticles on other fruits, crops, and agricultural products.

AUTHOR INFORMATION

Corresponding Author

*Food Science Program, Division of Food System & Bioengineering, University of Missouri, Columbia, MO 65211, USA. Tel: (573)884-6718; Fax: (573)884-7964. E-mail: linme@missouri.edu.

Funding

This research was supported by the USDA NIFA Nanotechnology Program Project No. 2011-67021-30391.

Notes

The authors declare no competing financial interest.

ACKNOWLEDGMENTS

We acknowledge the assistance from the Electron Microscopy Core facility at the University of Missouri in electron microscopy analysis.

REFERENCES

(1) FAO. 2012. Global pact against plant pests marks 60 years in action. Food and Agriculture Organization of the United Nations. http://www.fao.org/news/story/en/item/131114/icode/ (Accessed date: October 16, 2012).

(2) Strange, R. N.; Scott, P. R. Plant disease: A threat to global food security. *Annu. Rev. Phytopathol.* **2005**, *43*, 83−116.

(3) Carvalho, F. P. Agriculture, pesticides, food security and food safety. *Environ. Sci. Policy* **2006**, *9*, 685−692.

(4) Bergeson, L. L. Nanosilver: US EPA's pesticide office considers how best to proceed. *Environ. Qual. Manage.* **2010**, *19*, 79−85.

(5) Bouwmeester, H.; Dekkers, S.; Noordam, M. Y.; Hagens, W. I.; Bulder, A. S.; De Heer, C.; Ten Voorde, S. E. C. G.; Wijnhoven, S. W. P.; Marvin, H. J. P.; Sips, A. J. A. M. Review of health safety aspects of nanotechnologies in food production. *Regul. Toxicol. Pharmacol.* **2009**, *53*, 52−62.

(6) Magnuson, B. A.; Jonaitis, T. S.; Card, J. W. A Brief Review of the Occurrence, Use, and Safety of Food-Related Nanomaterials. *J. Food Sci.* **2011**, *76*, R126−R133.

(7) Kammer, F.; Legros, S.; Hofmann, T.; Larsen, E. H.; Loeschner, K. Separation and characterization of nanoparticles in complex food and environmental samples by field-flow fractionation. *TrAC, Trends Anal. Chem.* **2011**, *30*, 425−436.

(8) Tiede, K.; Boxall, A. B. A.; Wang, X.; Gore, D.; Tiede, D.; Baxter, M.; David, H.; Tear, S. P.; Lewis, J. Application of hydrodynamic chromatography-ICP-MS to investigate the fate of silver nanoparticles in activated sludge. *J. Anal. At. Spectrom.* **2010**, *25*, 1149−1154.

(9) Murdock, R. C.; Braydich-Stolle, L.; Schrand, A. M.; Schlager, J. J.; Hussain, S. M. Characterization of nanomaterial dispersion in solution prior to in vitro exposure using dynamic light scattering technique. *Toxicol. Sci.* **2008**, *101*, 239−253.

(10) Tiede, K.; Boxall, A. B. A.; Tear, S. P.; Lewis, J.; David, H.; Hassellöv, M. Detection and characterization of engineered nanoparticles in food and the environment. *Food Addit. Contam.* **2008**, *25*, 795−821.

(11) Feng, X.; Mao, C.; Yang, G.; Hou, W.; Zhu, J. J. Polyaniline/Au composite hollow spheres: synthesis, characterization, and application to the detection of dopamine. *Langmuir* **2006**, *22*, 4384−4389.

(12) Zhao, T.; Fan, J.-B.; Cui, J.; Liu, J.-H.; Xu, X.-B.; Zhu, M.-Q. Microwave-controlled ultrafast synthesis of uniform silver nanocubes and nanowires. *Chem. Phys. Lett.* **2011**, *501*, 414−418.

(13) Chen, G.; Wang, Y.; Tan, L. H.; Yang, M.; Tan, L. S.; Chen, Y.; Chen, H. High-purity separation of gold nanoparticle dimers and trimers. *J. Am. Chem. Soc.* **2009**, *131*, 4218−4219.

(14) Tighe, M.; Lockwood, P.; Wilson, S.; Lisle, L. Comparison of digestion methods for ICP-OES analysis of a wide range of analytes in heavy metal contaminated soil samples with specific reference to arsenic and antimony. *Commun. Soil Sci. Plant Anal.* **2004**, *35*, 1369−1385.

(15) De la Rosa, G.; Peralta-Videa, J.; Gardea-Torresdey, J. Utilization of ICP/OES for the determination of trace metal binding to different humic fractions. *J. Hazard. Mater.* **2003**, *97*, 207−218.

(16) Ikem, A.; Nwankwoala, A.; Odueyungbo, S.; Nyavor, K.; Egiebor, N. Levels of 26 elements in infant formula from USA, UK, and Nigeria by microwave digestion and ICP-OES. *Food Chem.* **2002**, *77*, 439−447.

(17) Delie, F. Evaluation of nano- and microparticle uptake by the gastrointestinal tract. *Adv. Drug Delivery Rev.* **1998**, *34*, 221−233.

(18) Sondi, I.; Salopek-Sondi, B. Silver nanoparticles as antimicrobial agent: a case study on *E. coli* as a model for Gram-negative bacteria. *J. Colloid Interface Sci.* **2004**, *275*, 177−182.

(19) Pal, S.; Tak, Y. K.; Song, J. M. Does the antibacterial activity of silver nanoparticles depend on the shape of the nanoparticle? A study of the gram-negative bacterium *Escherichia coli*. *Appl. Environ. Microbiol.* **2007**, *73*, 1712−1720.